

Implications of Site-Specific Conditions on the Prediction of Loading and Power Performance of a Tidal Stream Device

Graeme McCann

graeme.mccann@garradhassan.com

Mat Thomson

mat.thomson@garradhassan.com

Stuart Hitchcock

stuart.hitchcock@garradhassan.com

Garrad Hassan and Partners Ltd,

St Vincent's Works

Silverthorne Lane

Bristol

BS2 0QD

UK

Abstract

The aim of this paper is to investigate the implications of site-specific conditions on the prediction of loading and power performance of a tidal stream device.

The design tool GH Tidal Bladed is used to model a generic 2MW turbine operating at a location within EMEC's tidal test site. Data collected at the site is analysed to evaluate the tidal flow characteristics, including annual mean flow distribution, typical velocity profiles and turbulence intensities. The coherent structure of the turbulence is estimated by spectral analysis of ADCP data, although the assessment is limited, it provides some understanding of the turbulent length-scales and suggests that a von Karman model can be used to extrapolate measured data to generate a 3D time history of the flow field. The application of such a model is discussed. A review of nearshore/site wave data is used to estimate a wave scatter diagram at the site.

Using site characteristics two forms of analysis are conducted. The first evaluates the impact of turbulent flow and waves on structural loading and the second compares the variation in annual energy yield when incorporating measured site data.

An annual energy yield prediction is evaluated using time histories of the electrical power generation and the annual mean flow distribution. This value is compared to a simplified harmonic model, based on Admiralty data, and a steady and dynamic power curve prediction.

The need to evaluate the effect of turbulent flow and waves on structural loading is apparent. If cost-effective design solutions are to be achieved then it is a prerequisite to have a detailed description of the environmental conditions at a potential tidal turbine site - coupled with sophisticated, validated models which can incorporate the complex interaction of the environment with the operational behaviour of the turbine.

The potential importance of turbulent flow and waves on loading and performance underlines the requirement for detailed tidal flow measurement studies, followed by the development of validated spectral models of tidal current flow.

Keywords: Turbulence, wave, fatigue loading

Nomenclature

<i>CFRP</i>	Carbon fibre reinforced plastic
<i>D</i>	Diameter
<i>H_s</i>	Significant wave height
<i>hh</i>	Hub height
<i>i</i>	Stress range bin index
<i>I</i>	2 nd moment of area
<i>L</i>	Length of element
<i>L_i</i>	Stress range of <i>i</i> th bin
<i>L_N</i>	Stress range for <i>N</i> cycles
<i>m</i>	Inverse material SN slope
<i>M</i>	Bending moment
<i>MFS</i>	Mean fatigue strength (amplitude)
<i>r_i</i>	Radius (inner)
<i>r_o</i>	Radius (outer)
<i>T</i>	Wall thickness
<i>T_p</i>	Wave period
<i>TI</i>	Turbulence intensity
<i>TSR</i>	Tip speed ratio
<i>U</i>	Mean flow speed
<i>UCS</i>	Ultimate compressive strength
<i>V_{mnp}</i>	Mean spring peak current
<i>V_{mnp}</i>	Mean neap peak current
<i>λ</i>	Wavelength
<i>σ_l</i>	Axial stress

1. MOTIVATION

The development of tidal current turbines has reached the point where prototypes and pre-commercial devices are now, or are soon to be, operational. To make further progress into a fully-commercial phase it will be important for developers to use more sophisticated modelling techniques, as they seek both optimised design solutions and also certification and due diligence review of their products.

Sophisticated modelling of tidal current turbines must be able to accurately represent salient characteristics of both the turbine and also the environment in which it operates. The latter will clearly be of a site-specific nature, and it is the aim of this paper to demonstrate the effect of using realistic environmental conditions coupled with sophisticated modelling techniques.

Based on the findings, implications are drawn for the design and costs. Finally, general effects and patterns observed through the study are reported and discussed. Assessment and certification of a turbine with respect to the structure's integrity and safety, as well as to its power production, are applied to mitigate risks and to build confidence in the product's development and commercialisation. Third party assessment is often required by investors, insurers, operators and authorities - and to this end, certification agencies are already drafting guidelines for marine energy device certification [1]. Such guidelines invariably emphasize the need for detailed load analysis.

A detailed description of the environment in which tidal turbines are likely to operate, coupled with a sound understanding of how this environment interacts with the device, is required if its loading and performance is to be accurately predicted. The application of sophisticated modelling capabilities should thus accelerate the development of more optimised, cost-effective designs and lead to increased confidence in the industry.

This paper aims to quantify the importance of modelling realistic environmental conditions in the analysis of device loads and performance.

The results of this paper will be of interest to device designers concerned with understanding how sensitive their design is to variations in environment severity. It should also highlight how rigorous, detailed modelling of the device/environment interaction can reduce over-conservatism and facilitate more optimised design solutions.

2. METHODOLOGY

2.1. Data analysis and site characterisation

In any design basis or resource assessment, measurements of the site conditions should be used. As the location for many demonstrator devices, EMEC is a suitable candidate to use for this study. This section describes the methods used to analyse survey data as well as the method by which to construct the parametric models required for a loading and performance assessment.

2.1.1 ADCP data analysis

Two sets of ADCP data have been used. A typical low frequency sampling survey taken over 33.2 days and a high frequency 1 second sampling interval survey (made over 6.9 days) made at a nearby location. Both recorded at a depth bin size of 1m. The raw ADCP data has been processed and quality checked and, where possible, data correction methods based on linear interpolation have been applied to replace poor quality data points. The following data was produced:

- Flow probability distribution – is evaluated from the low frequency survey data. The mean flow speed bins used spanned from -0.2 to 3.8 m/s at a 0.4m/s spacing, (i.e. mid bin values of 0.0, 0.4, 0.8, 1.2, 1.6, 2.0, 2.4, 2.8, 3.2, 3.6).
- Flow probability distribution correlated to a long term measurement point – harmonic analysis of the low frequency survey data allows correlation with near long term tidal constituents, enabling a harmonic model to be used to produce a long term probability distribution.
- Flow direction - the hub height flow bin is analysed to assess the dominant flow directions.
- Vertical flow profile - flow bin data, normalised to hub height is used to characterise the typical profiles and evaluate power law fits.
- Flow turbulence intensities – ten minute running means from the high frequency survey data were used to establish mean and standard deviations.
- Flow turbulence structure and coherence, ADCP data cannot be used to establish the blade scale turbulence lengthscales, however, typical larger lengthscales may be inferred from spectral analysis.

2.1.2 Wave data analysis

The distribution of wave states (or wave spectrum) at any site is described using a wave scatter diagram. A MET Office offshore wave scatter diagram, for a model node located within 10 nautical miles of the site, is used as a basis. The results of nearshore transition models coupled with the offshore scatter diagram were used to create a nearshore scatter diagram.

2.2. GH Tidal Bladed

The effect of various environments on the loading of a generic horizontal axis tidal current turbine is assessed by simulating the device/environment behaviour and interaction using the industrial design tool, GH Tidal Bladed [2].

Tidal Bladed facilitates integrated, time-domain simulations which account for the complexities associated with, for example, unsteady flow fields, turbine structural dynamics, controller dynamics and rotor hydrodynamics. Tidal Bladed shares much of the same computational basis as GH Bladed, which has become an industry standard design tool in the analysis of offshore wind turbines [3]. In addition, Tidal Bladed has undergone its own validation study [4].

A number of assumptions were made when using Tidal Bladed

- A generic 2MW pitch-regulated, variable speed tidal turbine model was used for all simulations. A description of the model is provided in Section 3.1.
- Flow profiles are defined using a power law to describe the sub-sea flow. In addition, near surface wind-induced currents can also be applied. Although in this analysis the penetration of the wind-driven flow is assumed not to affect the rotor swept area.

- The turbulence flow fields were created from one of three 15 min samples of real high frequency flow data (measure at hub height). The first sample captures the turbulence of the current at slack water and the second captures the mid-flood point of the tidal cycle. The third sample is taken when the tidal cycle is at its peak velocity. A three dimensional turbulence flow field is created using the sampled time series as the longitudinal component of flow variation at the hub which is then extrapolated in the lateral and vertical dimensions using the improved von Karman model¹.
- A JONSWAP wave spectrum was applied in all stochastic sea-state simulations.
- There are several wave/current interaction models available for use within Tidal Bladed. However, the preferred option is always to have site-specific measurements. In lieu of this it is assumed for fatigue analysis that the current effect is averaged out over the turbine life span and effectively the nearshore spectrum is independent of the current. For the extreme event simulation the regular wave conditions are assumed to originate offshore. As a result, the wave lengths are altered due to the presence of the current. More detailed analysis of the site-specific wave climate and research is required to properly address the wave/current interaction complexities.
- Wind loadings are assumed small on the surface piercing structure.

2.3. Loading assessments

To compare the effect of both the environment and the modelling approaches, two loading assessment studies were conducted:

- Extreme event assessment – using the 10 year storm as a typical extreme event, the turbine’s dynamic controller responses to an extreme sea-state, incorporating sheared flow, turbulence and waves.
- Fatigue assessment analysis - operational fatigue load simulations were modelled in accordance with the GL draft guidelines for Ocean Energy Converters [1].

Both are compared with the steady state load².

2.4. Energy yield assessments

Several different energy yield modelling techniques were studied and compared:

- Steady state power curve, evaluated from blade element momentum theory coupled with a flow probability distribution evaluated from Admiralty data (e.g. V_{msp} , V_{mnp} ebb/flood) and a simplified harmonic tidal flow model.
- Steady state power curve and a flow probability distribution taken directly from 32 days of site measurements.
- Steady state power curve and a flow probability distribution constructed from site measurements and correlated to a long term measurement point.
- In lieu of a measured power curve, a dynamic power curve is taken from Tidal Bladed fatigue simulations and a flow probability distribution constructed from site measurements and correlated to a long term measurement point.

3. DATA ANALYSIS AND SITE CHARACTERISATION

3.1. Data analysis

Data quality control checks identified areas of erroneous data. As expected, a lot of poor data points were observed at or near the free surface. To avoid large areas of bad data the top 15 bins have been discarded. As the wave climate has not been assessed using the ADCP data then this loss of data is considered acceptable.

3.2 Flow probability distribution

Depth averaged³ and hub height flow speeds from the measured data are compared in the figure below. The close alignment demonstrates that the hub height depth bin is generally representative of the water column. In addition a simplified harmonic model distribution (using chart data [2]) has been evaluated at hub height along with the correlated long term measurement distribution.

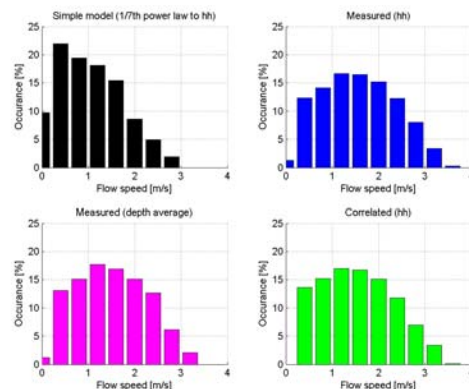


Figure 1: Probability distributions

The local port of Kirkwall is used as the long term measurement point to which the measured tidal harmonic constituents are correlated to. A harmonic model is adjusted to match the measured data in the appropriate frequency range. Figure 1 shows that the long term measurement results yield a slight variation to the

¹ The improved von Karman model is a wind turbulence model and is used to estimate the lateral and vertical turbulence lengthscales in the absence of appropriate site data.

² Steady state load is derived directly from blade element momentum theory.

³ Mean value of depth bins 2 to 40.

measured data (overpredicting slack water). Figure 2 compares the harmonic analysis.

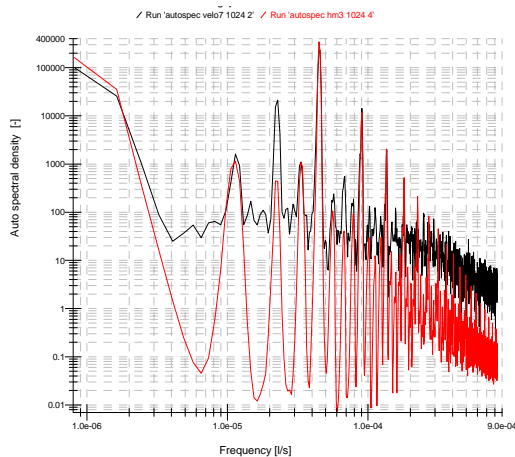


Figure 2: Harmonic analysis

3.2. Flow direction

Using the hub height time series for the low frequency data, the directional phase is shown below:

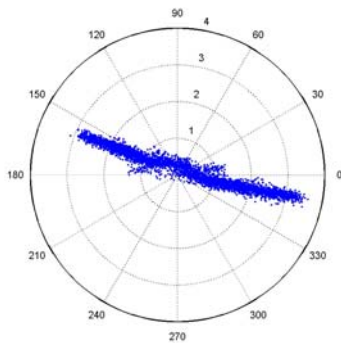


Figure 3: Polar plot of hub height flow speed

As illustrated in the figure above the dominant flow directions are 160 and 350 degrees. Generally the directional spread is less than 10 degrees, and more pronounced at lower flow speeds.

3.3. Characterisation of the velocity profile

For each flow speed bin, the mean flow speed at each depth bin is normalised to hub height flow speed and plotted against channel depth, providing typical vertical profiles for each flow speed bin. The plot below shows the normalised profiles. Fitting provides power law exponents.

Figure 4 plots power law fits to the average flow speed at each depth bin for each flow speed bin (where n is the power exponent). It shows that typically the flow exhibits a consistent profile ($\sim 1/5^{\text{th}}$ power law). As expected at very low flow speeds the profile tends to become flatter, but less uniform and a power law fit is not representative.

The original data does show a significant deficit near the free surface at $\sim 5\text{m}$ below the surface. This data was removed as part of the poor data set. The impact of this is insignificant but should be noted.

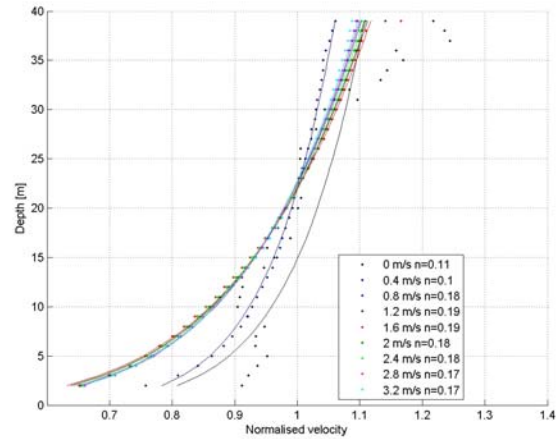


Figure 4: Flow profiles

3.3. Analysis of turbulence intensities & coherent lengthscales

Taking 10 min statistics (mean and standard deviation) of the high frequency data at hub height yields the relationship between flow speed turbulence intensity and the mean flow speeds through typical tidal cycles.

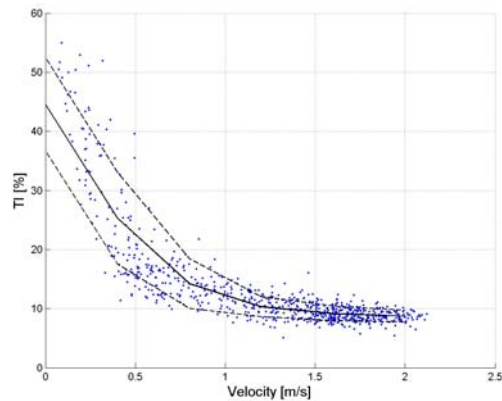


Figure 5: Flow turbulence intensity vs mean flow speed

Assuming that the high frequency ADCP sample is representative of normal flow conditions then Figure 5 demonstrates that the relationship between mean flow speed and flow turbulence intensity follows that of typical naturally occurring time varying boundary layer flow (and is somewhat similar to the wind conditions that a wind turbine might experience). The table below analyses three particular points in the tidal cycle:

Table 1: Flow turbulence through the tidal cycle

Description	Units	Sample		
		Slack water	Mid flow	Peak flow
Mean for sample	m/s	0.818	1.597	1.882
Turbulence intensity (Ix)	%	17.7	11.5	10.1

Spectral analysis of the data aims to highlight typical turbulence lengthscales. The frequency range of interest is much higher than that required for a harmonic analysis, typically in the range of $1e-3$ to 1 Hz. However, there is a limit to the usefulness of the ADCP data, due to the method by which it calculates the flow velocity. ADCP

instruments use three angled acoustic beams to evaluate the flow velocity at each bin depth. As a result the sample volume increases with distance from the instrument. At hub height the sample size has a diameter of ~15m, which at the highest flow speed correlates a cut-off frequency of 0.13Hz.

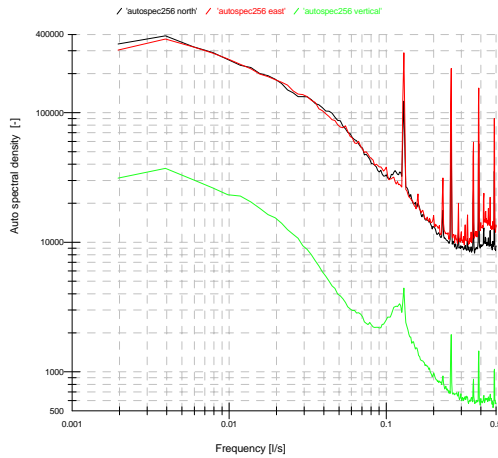


Figure 6: Measured velocity spectrum

The spectrum in Figure 6 indicates Kolmogorov’s spectral density description is observed after about 0.04Hz. As this point corresponds to a length scale similar to the water column it appears no larger scale lateral eddies are dominant. This could be expected given the local geography. The spiky peaks are errors associated with the ADCP and the hump at around 0.12Hz corresponds to the typical wave periods.

3.4. Review of wave climate

Based on site understanding it was assumed that the waves were predominately bi-directional and inline with the current direction. It was also assumed that two thirds originated from the northerly direction. The table below shows the constructed scatter diagram.

This table provides an indication of how the offshore wave climate might transfer to the site. Although the site is not particularly shallow the transition to nearshore is dependant on the local geography. The effect of the current will also have a major impact.

Table 2: Assumed wave scatter diagram

Hs (m)	Tz (s)						
	1.5	2.5	3.5	4.5	5.5	6.5	7.5
0.25	7.14	0.69	0.10				
0.75		26.78	27.16	0.58	0.03		
1.25			9.39	2.10	0.28	0.05	
1.75			0.79	8.09	5.83	0.06	0.02
2.25			0.02	2.05	2.97	1.05	0.19
2.75				0.31	2.31	1.20	0.26
3.25					0.22	0.25	0.07

3.5. Extreme event conditions

Through consultation with the tidal stream industry some typical extreme conditions have been suggested for the EMEC site, these are tabulated below:

Table 3: Extreme load case – 10 year wave event

Max flow speed [m/s]	4.1
Extreme flow turbulence [%]	10
10 yr wave [m, s]	9, 9

4. SIMULATIONS

4.1. Generic Tidal Turbine Model

A 2MW pitch-regulated variable speed generic turbine model is used for all simulations. The salient details of the model are summarised in Table 4.

Table 4: Generic turbine specification

Rated power [MW]	2.0
Rotor diameter [m]	22.8
Blade length [m]	10.5
Number of blades [.]	3
Rated hub flow speed [m/s]	3.0
Rated rotor speed [rpm]	12.0
TSR below rated [.]	5.8
Hub height above sea-bed [m]	22.0
Control type	Pitch regulated, variable speed
Transmission	Gear box
Support structure type	Bottom-mounted tripod
Foundation stiffness	rigid

Figure 7 shows how the steady power output [MW] (black), rotor speed [rad/s] (red), rotor thrust [MN] (green), blade root out-of-plane bending moment [MNm] (light blue), and pitch angle [rad] (blue) vary with flow speed (range: 0-4 [m/s]).

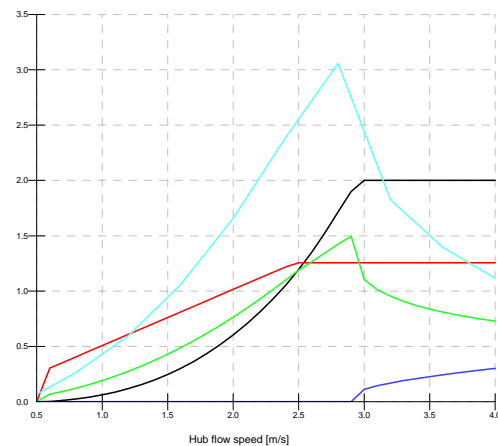


Figure 7: Steady plot as function of flow speed

The turbine is supported by a bottom-mounted steel tripod construction. The nacelle housing the turbine’s drive train attaches to the structure 22m above the sea-bed. The structure penetrates the sea-surface by 5m for a mean sea level of 50m (i.e. the structure is 55m high). Figure 3 depicts the configuration graphically.

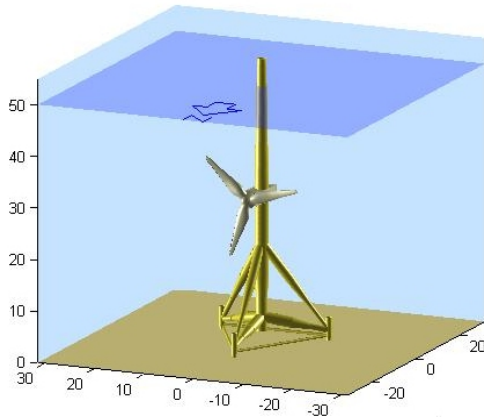


Figure 8: Generic tidal turbine model – ISO view

- All simulations were run for 10 minutes.
- Potential flow tower shadow.
- Rotor mass & geometric imbalance.
- Structural dynamics of the support structure are included but the rotor blades are assumed to be rigid as a first approximation.
- Current shear using power law.
- Turbulence files use measured data at hub height normalised to the mean flow speed for each flow bin (see Section 2.2. & Table 1). Characteristic lengthscales correspond with observations.

Figure 9 compares the spectral analysis of the measured data and a typical von Karman model output. There is more energy associated with the model data due to the exploitation to a greater flow speed for the purpose of the fatigue analysis. In the sub-inertial region the model compares well with the measured data, but the von Karman model appears to predicting several dominate lengthscales as compared to the data.

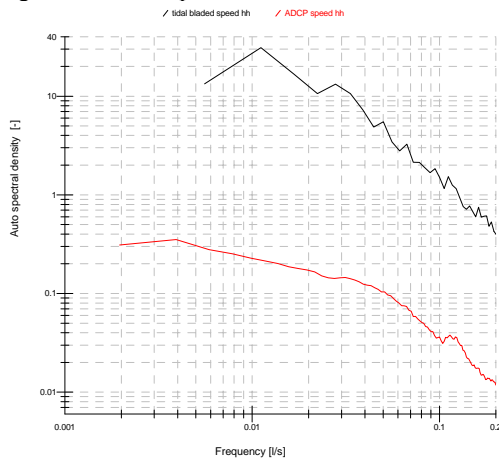


Figure 9: Modelled and measured speed spectrum

4.2. Simulation set-up

For the extreme event simulation the following attributes are used:

Table 5: Extreme load case – 10 year wave event

Rated flow speed [m/s]	3.5
Extreme flow turbulence [%]	10
Extreme stream fn wave H, T [m, s]	9, 9
Wave, current direction	In line
Wave current interaction	λ shift

To conduct a thorough fatigue analysis a simulation of all possible environmental permutations is required. To achieve this all sea states should be sampled at each flow speed. Flow distribution (Figure 1) and constructed wave scatter diagram were used for fatigue analysis (Table 2). In addition the direction of the wave and currents is important when considering the wave/current interaction.

Table 6: Fatigue simulation set up

		Head-on		In-line	
		North -10°	South +10°	North -10°	South +10°
Current	Heading				
	Probability (occurrence)	50%	50%	50%	50%
	No of bins	9		9	
Waves	Heading	South +10°	North -10°	North -10°	South +10°
	Probability (occurrence)	37%	63%	63%	37%
	No of bins	28		28	
Total	Probability (occurrence)	19%	31%	31%	19%
	No of bins	252		252	

Utilising the multiple set up function within Tidal Bladed 480 simulations⁴ were constructed to capture the full extent of the varying environmental states.

4.3. Fatigue simulation post processing

Each simulation is integrated over the turbine lifetime to provide lifetime Damage Equivalent Loads (DELs), which are used to equate the fatigue damage, represented by rain flow cycle counted data, to that caused by a single stress range repeating at a single frequency (in this case the equivalent load frequency equates to 10e7 cycles in 20 years (0.158Hz)). The damage equivalent stress is given by the following formula:

$$L_N = \sqrt[m]{\frac{\sum L_i^m n_i}{N}} \quad \{eqn 1\}$$

where L_N is the equivalent stress for N cycles L_i is the stress range bin i . n_i is the number of rain flow cycles at stress range bin i . m is the negative inverse of the slope on the material's Wöhler curve (m is also referred to as the S-N curve slope). N is the number of cycle repetitions in the turbine lifetime.

The stress, L_i , depends upon the geometry of the structure under consideration. It is assumed that stress is

⁴ 2x12 simulations discarded on the grounds of negligible occurrence

proportional to load, therefore it is quite acceptable to use load instead of stress in the above equation.

5. LOADING ASSESSMENTS

Figure 7 provides the steady state peak blade root out-of-plane bending moment (M_y) at 3057kNm.

In Figure 10 the time-history simulation results for the extreme load case are presented in terms of the following salient variables:

- Hub flow speed [m/s] – (black)
- Sea surface elevation [m] – (red)
- Blade 1 pitch angle [rad] – (green)
- Blade 1 root out-of-plane bending moment, M_y [MNm]– (blue)
- Rotor thrust, F_x [MN] – (light-blue)

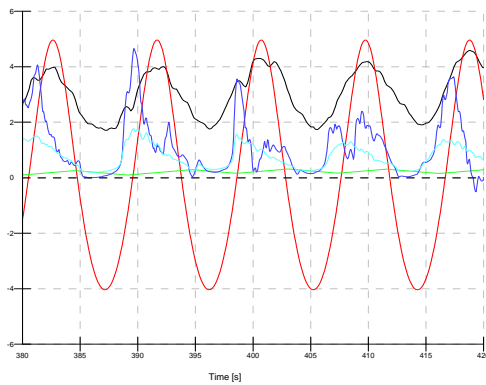


Figure 10: Extreme load simulation time series

From the results of the simulation the maximum blade root out-of-plane bending moment M_y , is 4657kNm (before the application of safety factor).

The fatigue analysis yields a typical rain flow diagram, as shown in Figure 11 below.

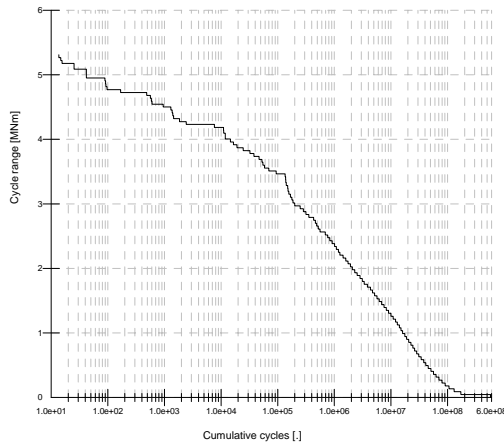


Figure 11: My rainflow plot of SN14

The corresponding M_y DEL for SN slope 14 is 2379kNm.

To facilitate a simple case for comparison of extreme and fatigue loading, the blade root component is modelled as

a simple cylindrical section of constant wall thickness. It has been assumed that the component is constructed from CFRP, with the following material properties [6]:

Table 7: Material properties of CFRP

Property	Unit	Value
Specific gravity	n/a	1.58
Young's Modulus	GPa	142
UCS	MPa	1105
MFS* (10e7 cycles)	MPa	350

* corresponding to a material inverse-SN slope = 14

The geometry of the component is represented by a cylinder where r_o is the outer radius and r_i is the inner radius.

The following relationships can thus be stated:

$$D = 2.r_o \quad \{eqn 2\}$$

$$T = r_o - r_i \quad \{eqn 3\}$$

$$I = \pi.[D^4 - (D-2.T)^4]/64 \quad \{eqn 4\}$$

$$\sigma_1 = M.r_o/I \quad \{eqn 5\}$$

To assess fatigue load criticality, the component is firstly dimensioned such that a zero reserve margin in *extreme* yield stress is achieved when applying a safety factor of 1.35 to the extreme load case maximum value of M_y , ie:

$$1.35.\sigma_1/\sigma_{UCS} = 1 \quad \{eqn 6\}$$

For Equation 6 to be satisfied, a feasible solution is:

$$D = 1.0m, T = 7.0mm$$

(Note, these dimensions have been determined purely on the basis of axial yield stress – a rigorous design process would include consideration of extreme buckling failure in addition).

It is now possible to calculate fatigue stress reserve margins for the simplified blade root component, based upon the DEL and the component's geometric and material properties.

Table 8: Loading assessment results

Load assessment	M_y load [kNm]	Ratio to steady load	Stress margin to extreme load
Steady state	3057.78	-	-
Extreme load case	4657.22	1.52	-
Fatigue DEL	2378.59	-	0.37

In this analysis the design driving load is the extreme load case. It is clear that without considering the numerous dynamic affects the design load could be 50% higher. In this particular case the fatigue loads don't drive the design, however, only one component of the turbine has been considered here.

6. ENERGY YIELD ASSESSMENT

Prior to using the measured probability distributions, illustrated in Figure 1, the flow speed bins are checked to ensure they are representative of flow samples within

each bin. The figure below compares the mean bin flow speed to the mid-bin flow value (as listed in Section 2.1.1). The plot indicates fairly good agreement, however, for a proper energy and fatigue assessment more bins would be utilised to ensure the bins don't induce an overestimation of yield or an underestimation in turbulence intensity for a given flow speed.

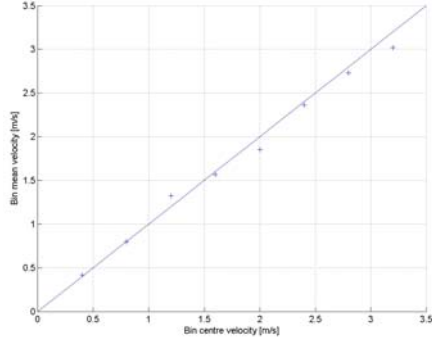


Figure 12: Average bin value vs mid bin value for measured data

The dynamic power curve is taken from fatigue simulations. It incorporates the effect of a dynamic controller, which will sacrifice energy yield for power quality during turbulence flow. The effect of this is most pronounced around the knee of the power curve.

Combining the different probability distributions in Figure 1 with one of the two power curves in Figure 13 enables a selection of annual energy predictions to be made (no reduction due to device availability is made). The results are presented in Table 9.

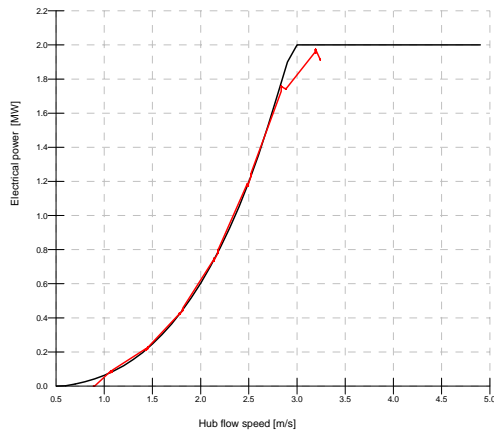


Figure 13: Steady state (black) and dynamic (red) power curves

Even though the reference Admiralty data used is associated with a nearby location, the spatial variation in flow is such that the annual energy yield prediction is much lower than for the prediction made with the measured data.

Table 9: Energy Load assessment results

Approach	AE yield (GWh p.a.)	Ratio
Steady state power curve and simplified tidal model	1.84	0.4
Steady state power curve and measured data	4.42	1.1
Steady state power curve and a freq distribution correlated to a long term measurement point.	4.21	1.0
Dynamic power curve and a freq distribution correlated to a long term measurement point.	4.31	1.0

The variation between the measured data and long term correlated data is small. This is because the measured data seems to be fairly representative of the V_{msp} and V_{mnp} , such that the equinox variation does not bias the measured data. The dynamic power curve yields slight more energy at the lower, more frequently occurring flow speeds.

7. DISCUSSION

Points regarding site characterisation include:

- The flow profile plots show that the typically assumed 1/7th power law is not applicable at this site and that a greater shear profile exists. This will have a major impact on rotor loads, inducing a larger 1P fatigue load. At flows below cut-in a power law model is not applicable, however this is of negligible effect.
- The level of ambient turbulence intensity is shown to be relatively high at 10% and given that the magnitude of the turbulence intensity has a major impact on fatigue loading, it highlights the need for proper representation of turbulence.
- The turbulent flow variations of interest are at the rotor sampling frequency. It is crucially important to understand the transfer of rotor load from low frequencies to those associated with the rotational speed and its harmonics. This can be a significant source of fatigue loading. However, ADCP data cannot be used to assess the turbulence length scales of interest. More work is required to properly analyse the turbulence structure, although from the limited analysis it suggests that the Kolmogorov law is applicable and that sensible turbulence flow fields can be simulated.
- For a proper fatigue load analysis, the site-specific wave climate should be required and ideally characterised as a function of the current speed. However, in lieu of quality data, a constructed scatter diagram has been used.

Points regarding loading assessment:

- A safety margin of 2 is required upon the steady state load to account for the dynamic effects of the extreme environmental conditions and the required design safety factor. In this analysis only one example of an extreme event is reviewed. In reality there are many load cases which have to be considered, including fault cases and other extreme events. Another possible

major event that might be considered is that of the constrained wave simulation, which simulates an extreme individual wave event in a random background sea state.

- In this analysis it was assumed that both the waves and current had two dominant directions. This is a key assumption when considering the number of fatigue simulations required. For the EMEC site it is a fair assumption, however, other sites vary - potentially leading to a very large number of simulations.
- The generic turbine used in this study was designed for sites where with the flow speed regularly exceeds the rated hub height flow speed of 3.0m/s. In this study the site conditions were such that this was not the case. As a significant amount of damage generally occurs around the rated flow point the fatigue loading in this study are much reduced.
- The study has shown that fatigue loading, although not driving in this particular example, is still an important design consideration and cannot be neglected. This view is reinforced by the fact that only one component of the turbine was considered in this study, which in reality is not likely to be the most sensitive to fatigue loading.

Points regarding the annual energy yield assessment include:

- The probability distributions generated by the simplified harmonic model using Admiralty data chart diamond data as input can be very misleading. A limitation of the harmonic model is the tendency for it to over predict the occurrence of slack water. Clearly for any serious project development (i.e. a bankable project) site-measured data will be required.
- In this assessment the size of flow bins was appropriate; however, for bankable projects greater accuracy will be required.
- Correlation to a long term data point is beneficial when the measured data is not representative of the yearly variation. For a bankable project this type of analysis should be considered, due to slight variations.
- Clearly the dynamic power curve is somewhat different from the steady-state curve and can have a major impact on yield. The supply of verified power curves will evidently be required in a proper resource assessment, but until such power curves are available, model simulations provide a viable alternative to demonstrate the effect of a highly variable flow environment on energy production.

8. CONCLUSIONS

The aim of this paper was to highlight the importance of understanding the specific environmental conditions at an installation site. Failure to incorporate detailed representation of the main environmental permutations can impact on both design and energy yield.

This analysis highlights that site data is critical for a proper design consideration. The degree to which the flow profile, direction, turbulence intensity and coherence structure, and wave climate are understood can have a major impact on the design.

The potential importance of flow turbulence underlines the requirement for detailed flow measurement studies, followed by the development of validated spectral models of tidal current flow. Nevertheless, this initial analysis suggests that the turbulence models developed for the wind turbine industry have some validity in modelling turbulent tidal flow fields.

Designers of a real turbine are encouraged to consider the conclusions of the study applied to such components as, for example, the gear box and support structure, in addition to the rotor. It would also be interesting to observe how the sensitivities of loading change if the rigid-structure assumption cannot be made and structural rotor dynamics are included.

9. REFERENCES

- [1] Germanischer Lloyd, Draft "Guideline for the Certification of Ocean Energy Converters, Part 1: Ocean Current Turbines", 2005.
- [2] Diamond C from Admiralty Chart C68, Cape Wrath to Wick and the Orkney Islands, Printed by Imray Laurie Norie and Wilson Ltd.
- [3] Bossanyi E A, "GH Tidal Bladed Theory Manual", GH & Partners Ltd, 2007.
- [4] Bossanyi E A, "GH Bladed Theory Manual", GH & Partners Ltd, 2003.
- [5] Bahaj et al, "Experimental verifications of numerical predictions for the hydrodynamic performance of horizontal axis marine current turbines", WVEC 2006.
- [6] Argyriadis K., Schwartz S. "Certification of Ocean Current Turbines, the GL Wind Guideline", Proceedings of World Maritime Technology Conference, MAREC, 2006.
- [7] Burton et al, "Wind Energy Handbook", Wiley 2001.

ACKNOWLEDGEMENT

GH kindly thanks EMEC for the timely supply of the ADCP data and TGL for their advice on the typical wave climate and expected extreme events at the EMEC site.